

Jet Noise Prediction Using Turbulent Scales from LES and RANS

Shabeeb N. P.¹ and Aniruddha Sinha¹

¹Department of Aerospace Engineering, IIT Bombay, Mumbai 400076, India

ABSTRACT

This paper studies the modelling of turbulent scales used in an existing steady Reynolds averaged Navier-Stokes solution-based acoustic analogy. The turbulence in the flow has been described as a statistical model of the two-point cross-correlation of the velocity fluctuations, characterized by the turbulent length and time scales. The modelling of the turbulent length and time scales from the $\overline{K} - \bar{\epsilon}$ data used in the steady RANS-based acoustic analogy has been validated with those computed from the cross-correlation of the velocity fluctuations. This was pursued with an LES database comprising an isothermal and a heated ideally-expanded Mach 1.5 round jets. The far-field noise has been computed using the turbulent scales from both the cross-correlation data and the $\overline{K} - \bar{\epsilon}$ data. The two results agree very well, and also display reasonable match with direct predictions from the time-resolved LES data using the Ffowcs Williams-Hawkings method.

Keywords: Aeroacoustics, jet noise prediction, noise source modelling

I. INTRODUCTION

Jet noise is one of the most challenging fluid mechanics problems that researchers have been working on for the last few decades. It is also one of the loudest noises ever produced by mankind. Jet noise consists of turbulent mixing noise, broadband shock associated noise (BBSAN) and screech tones [1]. The latter two noise components are generated only in supersonic jets when the jet is imperfectly expanded and a shock cell structure is formed in the jet plume. The turbulent mixing noise is the dominant component of the jet noise which is generated by the mixing of the jet with the ambient air. We focus only on the turbulent mixing noise in this paper.

The approach to jet noise prediction has the following elements to it. The designation of a noise source and propagation operator, either calculation or modelling of the noise sources, and solution of the radiated sound. But there is no clear separation of noise from the rest of the flow and there is no unique designation for the noise source. So there are numerous possible choices for decomposing the flow equations, written compactly here for flow field vector q as $N(q) = 0$, into a noise source \mathcal{S} and a propagation operator L as $Lq = \mathcal{S}(q)$. This is an exact reformulation, and it is known as an acoustic analogy. The first such theoretical formulation for aerodynamic noise prediction was the work of Lighthill [2]. Lighthill's formulated his analogy by reworking the Navier-Stokes equation (NSE) itself. He chose

the propagator L as the free-space wave operator and the source took on a quadrupolar character. Lilley [3] modified Lighthill's equation by considering the propagation of sound through a locally-parallel medium, as is appropriate for many shear flows, and jets in particular. Later, Ref. [4] proposed a generalized acoustic analogy that was an exact consequence of NSE considering the propagation of sound through an arbitrary medium. These successive developments are geared towards shifting the burden from modelling of the source \mathcal{S} to solving the wave operator L .

The direct prediction of the noise generated and radiated by a turbulent flow using Direct Numerical Simulation (DNS) or Large Eddy Simulation (LES) is computationally expensive and time-consuming. Ref. [5] proposed a semi-empirical theory to predict the far-field noise from fine-scale turbulence that required minimal information from a CFD database. This model required only the mean flow velocity, density, turbulent kinetic energy and dissipation in the near-field region. The much more economical steady Reynolds averaged Navier-Stokes (RANS) simulation sufficed for this purpose. The turbulent statistics in the source region were modelled using the turbulent length scales, time scales and velocity scales. The authors showed very accurate noise prediction vis-à-vis experimental measurements over a wide range of jet velocities and temperature ratios for single-stream round jets, especially in the sideline and upstream direction where the fine-scale contribution dominates. Refs. [6] and [7] introduced an acoustic analogy based on the linearized Euler equations (LEE) with no assumptions of fine-scale or large-scale noise sources. This approach was also used in Ref. [8] for a Mach 0.9 jet, where comparisons were made with the noise results from the asymptotic solutions given in Refs. [9] and [10]. Miller [11] presented an acoustic analogy that independently predicted the noise from turbulent mixing and shock interactions based on the LEE. Of late, this methodology has been successfully used to predict the noise from chevron jets and axisymmetric dual-stream jets for a wide range of Mach numbers and temperature ratios; it is employed in the present work too.

In all the steady RANS-based acoustic analogies, the local turbulent length and time scales are modeled from local $\overline{K} - \bar{\epsilon}$ data using simple scaling laws and empirical coefficients. In this work, we investigate the accuracy of these models by comparing them with the length and time scales computed directly from the cross-correlation of the velocity fluctuations found in a well-validated LES database [12] comprising of two supersonic round jets – one isothermal and the other heated. In essence, we extract the relevant time-averaged quantities from the LES data, and use only these as

input to the RANS-based acoustic analogy model. We find that, although there are some discrepancies in the modeled scales, the predicted far-field sound from both inputs closely match the sound propagated directly from the time-resolved LES data using the Ffowcs Williams - Hawkings (FW-H) approach.

II. PREDICTING JET NOISE FROM RANS

The acoustic analogy presented here is based on the works of Refs. [5–8, 11]. We start from the Euler equations as viscous effects are unimportant for both sound generation and propagation. The equations are

$$\frac{D\pi}{Dt} + \nabla \cdot \mathbf{u} = 0, \quad (1a)$$

$$\frac{D\mathbf{u}}{Dt} + a^2 \nabla \pi = 0. \quad (1b)$$

where $D(\cdot)/Dt$ is the material derivative and $\pi := (1/\gamma) \ln(p/p_\infty)$. These are rewritten by expanding the flow variables as fluctuations on a time-averaged base state and retaining terms on the left hand side (LHS) that are linear in the fluctuations while gathering all remaining terms in the right hand side (RHS). The consequent forced LEE is:

$$\frac{\overline{D}\pi'}{\overline{D}t} + \nabla \cdot \mathbf{u}' = -\mathbf{u}' \cdot \nabla \pi' =: f_0, \quad (2a)$$

$$\frac{\overline{D}\mathbf{u}'}{\overline{D}t} + \mathbf{u}' \cdot \nabla \bar{\mathbf{u}} + \overline{a^2} \nabla \pi' = -\mathbf{u}' \cdot \nabla \mathbf{u}' - (a^2)' \nabla \pi' =: \mathbf{f}, \quad (2b)$$

where $\overline{D}(\cdot)/\overline{D}t := \partial(\cdot)/\partial t + \bar{\mathbf{u}} \cdot \nabla(\cdot)$. The nonlinear terms on the RHS are the noise sources; specifically, f_0 is the unsteady dilatation and \mathbf{f} is the unsteady force per unit mass. For free jets, the mean pressure is generally taken to be the ambient value (i.e., $\bar{p} = p_\infty$). Also, $\pi' \approx \pi = \gamma^{-1} \ln(1 + p'/p_\infty) \approx \gamma^{-1} p'/p_\infty$. The solution to the inhomogeneous equation can be determined by finding its Green's function.

Considering a locally parallel mean flow, we arrive at the following formulation of the forced LEE in cylindrical coordinates $\mathbf{x} := (x, r, \phi)$ in the frequency domain:

$$\overline{D}_\omega \hat{\pi} + \frac{\partial \hat{u}_x}{\partial x} + \frac{1}{r} \frac{\partial(r\hat{u}_r)}{\partial r} + \frac{1}{r} \frac{\partial \hat{u}_\phi}{\partial \phi} = \hat{f}_0, \quad (3a)$$

$$\overline{D}_\omega \hat{u}_x + \frac{d\bar{u}_x}{dr} \hat{u}_r + \overline{a^2}(\mathbf{x}) \frac{\partial \hat{\pi}}{\partial x} = \hat{f}_x, \quad (3b)$$

$$\overline{D}_\omega \hat{u}_r + \overline{a^2}(\mathbf{x}) \frac{\partial \hat{\pi}}{\partial r} = \hat{f}_r, \quad (3c)$$

$$\overline{D}_\omega \hat{u}_\phi + \frac{\overline{a^2}(\mathbf{x})}{r} \frac{\partial \hat{\pi}}{\partial \phi} = \hat{f}_\phi, \quad (3d)$$

where $\overline{D}_\omega := -i\omega + \bar{u}_x \partial/\partial x$.

To make progress, the four periodic vector Green's

functions of the LEE are defined as the solutions of

$$\overline{D}_\omega \hat{\pi}_g^n + \nabla \cdot \hat{\mathbf{u}}_g^n = \delta(\mathbf{x} - \mathbf{x}_s) \delta_{0n}, \quad (4a)$$

$$\overline{D}_\omega \hat{u}_{g,x}^n + \frac{d\bar{u}_x}{dr} \hat{u}_{g,r}^n + \overline{a^2} \frac{\partial \hat{\pi}_g^n}{\partial x} = \delta(\mathbf{x} - \mathbf{x}_s) \delta_{xn}, \quad (4b)$$

$$\overline{D}_\omega \hat{u}_{g,r}^n + \overline{a^2} \frac{\partial \hat{\pi}_g^n}{\partial r} = \delta(\mathbf{x} - \mathbf{x}_s) \delta_{rn}, \quad (4c)$$

$$\overline{D}_\omega \hat{u}_{g,\phi}^n + \frac{\overline{a^2}}{r} \frac{\partial \hat{\pi}_g^n}{\partial \phi} = \delta(\mathbf{x} - \mathbf{x}_s) \delta_{\phi n}. \quad (4d)$$

Here, the vector Green's functions have the common arguments $(\mathbf{x}|\mathbf{x}_s; \omega)$ and are indexed by n , which takes values in $\mathcal{N} := \{0, x, r, \phi\}$. Basically, we are seeking the response at \mathbf{x} due to harmonic forcing at the location \mathbf{x}_s with ω . Moreover, the forcing is of a particular kind – either a volume source or one of the three components of a force source.

The vector LEE operator can be simplified to a third-order scalar operator acting on the most relevant component – viz. $\hat{\pi}_g^n$ – called the Lilley's operator:

$$\underbrace{\left(\overline{D}_\omega^3 - \overline{a^2} \overline{D}_\omega \nabla^2 - \frac{d\overline{a^2}}{dr} \overline{D}_\omega \frac{\partial}{\partial r} + 2\overline{a^2} \frac{d\bar{u}_x}{dr} \frac{\partial^2}{\partial x \partial r} \right)}_{L_L} \hat{\pi}_g^n = \overline{D}_\omega^2 (\delta(\mathbf{x} - \mathbf{x}_s)) \delta_{0n} - \overline{D}_\omega \frac{\partial}{\partial x} \delta(\mathbf{x} - \mathbf{x}_s) \delta_{xn} - \left[\frac{1}{r} \overline{D}_\omega \frac{\partial}{\partial r} (r\delta(\mathbf{x} - \mathbf{x}_s)) - 2 \frac{d\bar{u}_x}{dr} \frac{\partial}{\partial x} \delta(\mathbf{x} - \mathbf{x}_s) \right] \delta_{rn} - \frac{1}{r} \overline{D}_\omega \frac{\partial}{\partial \phi} \delta(\mathbf{x} - \mathbf{x}_s) \delta_{\phi n} =: \mathcal{S}^n(\mathbf{x} - \mathbf{x}_s; \omega). \quad (5)$$

Lilley's operator's (scalar) Green's function is such that

$$L_L \hat{g}(\mathbf{x}|\mathbf{x}_s; \omega) = \delta(\mathbf{x} - \mathbf{x}_s). \quad (6)$$

It turns out that it is much simpler to solve the adjoint problem and invoke reciprocity to arrive at \hat{g} [5]. With this in hand, the pressure component of the vector Green's function of LEE can be written as

$$\hat{\pi}_g^n(\mathbf{x}|\mathbf{x}_s; \omega) = \iiint \hat{g}(\mathbf{x}|\mathbf{x}_t; \omega) \mathcal{S}^n(\mathbf{x}_t - \mathbf{x}_s; \omega) d\mathbf{x}_t. \quad (7)$$

The pressure fluctuation is obtained by convolving the four Green's functions' pressure components with the corresponding source terms of the LEE. However, we are interested in (and cannot ask for more than) the spectral density of pressure. This is found as

$$\frac{S_p(\mathbf{x}, \omega)}{(\gamma p_\infty)^2} = \sum_{n, n' \in \mathcal{N}} \int_{\mathbf{x}_s} \hat{\pi}_g^{n*}(\mathbf{x}|\mathbf{x}_s; \omega) \int_{\mathbf{x}_s} \hat{\pi}_g^{n'}(\mathbf{x}|\mathbf{x}_s + \boldsymbol{\eta}; \omega) \times \int_{\tau} \langle f_n(\mathbf{x}_s, t) f_{n'}(\mathbf{x}_s + \boldsymbol{\eta}, t + \tau) \rangle e^{i\omega\tau} d\tau d\boldsymbol{\eta} d\mathbf{x}_s. \quad (8)$$

Thus, the necessary input for our approach is the mean flow field for computing the Green's functions and a model of the two-point-two-time cross-correlation of the nonlinear source terms of the LEE.

Based on extensive round jet databases accumulated over decades, such a model for the spatio-temporal cross-correlations of the source terms has been proposed by many researchers [5, 7, 13], and is of the form

$$\langle f_n(\mathbf{x}_s, t) f_{n'}(\mathbf{x}_s + \boldsymbol{\eta}, t + \tau) \rangle = \delta_{nn'} A_n(\mathbf{x}_s) e^{-|\tau|/\tau_s - (\eta_x - \bar{u}_x \tau)^2/\ell_x^2 - \eta_y^2/\ell_y^2 - \eta_z^2/\ell_z^2}, \quad (9a)$$

$$A_0 = B_0^2 \frac{(u_s/a_\infty)^4}{\tau_s^2}, \quad A_n = B_{>0}^2 \frac{(u_s/a_\infty)^2 u_s^4}{\ell_x^2}. \quad (9b)$$

where $n \in \{x, r, \phi\}$. At zero-time lag, this posits a Gaussian decay of the two-point cross-correlation in all directions, albeit with different length scales ℓ_x, ℓ_y, ℓ_z . Moreover, it invokes the frozen field hypothesis and posits an exponential decay of correlation with time having time scale τ_s , if one were to move with the mean flow (assumed negligible in the cross-stream directions for this purpose). Further, the model assumes that the four source terms (for the four equations) are uncorrelated. Finally, the magnitudes of the correlation functions are related by dimensional analysis to the local velocity scale u_s and the length and time scales.

The turbulent length scale is expected to depend on the frequency being considered. Let us denote the frequency-dependent streamwise length scale as $l_x(\mathbf{x}_s, St)$, where $St = \omega D_j / (2\pi U_j)$ is the Strouhal number corresponding to the frequency ω under consideration, D_j is the jet's nozzle-exit diameter, and U_j is its nozzle-exit velocity. Following Ref. [14], all these length scales are modeled as

$$l_i(\mathbf{x}_s, St) = l_i(\mathbf{x}_s) \frac{1 - e^{-c_f St}}{c_f St}, \quad \forall i \in \{x, r, \phi\}, \quad (10)$$

where $c_f = 11.25$ was chosen to match the experimental observations.

Assuming that the observer is in the far-field, the vector Green's function of two closely-placed source points differ by only a phase factor:

$$\hat{\pi}_g^n(\mathbf{x}|\mathbf{x}_s + \boldsymbol{\eta}; \omega) \approx \hat{\pi}_g^n(\mathbf{x}|\mathbf{x}_s; \omega) e^{-i(\omega/R/a_\infty)\mathbf{x} \cdot \boldsymbol{\eta}}, \quad (11)$$

where R is the polar radius of the observer (i.e., distance from the jet nozzle exit's center). Using this simplification, along with the specific model of the spatio-temporal correlation in eqn. (9), allows one to analytically evaluate the integral in eqn. (8) over the spatio-temporal lags (i.e., over $\boldsymbol{\eta}$ and τ) to arrive at

$$\frac{S_p(\mathbf{x}, \omega)}{(\gamma p_\infty)^2} = 2\pi^{3/2} \sum_{n \in \mathcal{N}} \int |\hat{\pi}_g^n(\mathbf{x}|\mathbf{x}_s; \omega)|^2 \sigma_n(\mathbf{x}_s; \omega, \mathbf{x}) d\mathbf{x}_s, \quad (12)$$

$$\sigma_n := A_n l_x l_y l_z \tau_s \frac{e^{-0.25\omega^2(l_x^2 \cos^2 \Theta + l_y^2 \sin^2 \Theta)/a_\infty^2}}{1 + \omega^2 \tau_s^2 (1 - \bar{u}_x \cos \Theta / a_\infty)^2}.$$

Here, Θ is the polar angle of the observer measured w.r.t. the jet downstream axis, and the local length scales are replaced by their frequency-dependent counterparts.

In the present work, we evaluate the following two alternate approaches to obtaining the necessary inputs to this noise prediction technique, which are the turbulent length and time scales.

A. Source Model 1

As mentioned at the outset, we are using an LES database of two supersonic round jets. In this first approach, we start out by calculating the local spatio-temporal cross-correlations of axial velocity fluctuations in the two jets. Then, we obtain the local length scales and time scales of an individual jet by fitting its spatio-temporal cross-correlation with the Gaussian-exponential ansatz of eqn. (9). Specifically, the local time scale $\tau_s(\mathbf{x})$ is determined by fitting with an exponential the peaks of the local two-point two-time cross-correlation data (i.e., $\eta_y = 0$ and $\eta_z = 0$, and η_x assumed to be $\bar{u}_x \tau$). The local axial length scale $\ell_x(\mathbf{x})$ is determined by fitting with a Gaussian the local cross-correlation data at finite streamwise separation and no separation in other coordinates (i.e., $\tau = 0$, $\eta_y = 0$ and $\eta_z = 0$). Following the literature, the cross-stream length scales are assumed to be one-third of the streamwise length scales at all locations:

$$\ell_y(\mathbf{x}) = \ell_z(\mathbf{x}) = \ell_x(\mathbf{x})/3. \quad (13)$$

Finally, the local velocity scale is determined from the local mean turbulent kinetic energy computed from the LES data again:

$$u_s(\mathbf{x}) = c_u \sqrt{2\bar{K}(\mathbf{x})}/3. \quad (14)$$

The free parameters for this model are c_u seen above, c_f appearing in eqn. (10) (and set as mentioned in its discussion), as well as the two amplitude constants B_0 and $B_{>0}$ present in eqn. (9). These last two are determined by best-fitting the noise data across the two jets (see Section III).

B. Source Model 2

In the second approach, we start by computing the local time-averaged values of turbulent kinetic energy $\bar{K}(\mathbf{x})$ and dissipation $\bar{\epsilon}(\mathbf{x})$ from the LES database. Then, the turbulent length and time scales are modeled as [5–8, 11]:

$$\ell_x = c_\ell \frac{(\bar{K})^{3/2}}{\bar{\epsilon}}, \quad \tau_s = c_\tau \frac{\bar{K}}{\bar{\epsilon}}, \quad u_s = c_u \sqrt{\frac{2}{3}\bar{K}} \quad (15)$$

where, c_ℓ, c_τ and c_u are constants. At each point within the jet plume, the cross-stream length scales are estimated from the streamwise one using eqn. (13) as before. Apart from these constants, c_f, B_0 and $B_{>0}$ also have to be set, just as in the first source model described above.

III. RESULTS AND DISCUSSION

A steady RANS solution is enough to predict the far-field jet noise using the model explained in the previous section. However, if we want to *validate* such a model, then we need an independent prediction of the noise, which is impossible with the RANS data. So, instead of using a steady RANS solution, the LES results of Brès et al. [12] are used, and the required input parameters are computed from it as described above for the two source models. The database comprises of an isothermal ideally-expanded round jet (case B118) and a heated ideally-expanded round jet (case B122), summarized in Table 1. The unstructured LES grid had 42 million control volumes; for the current analysis, this data

Table 1: Test cases used from LES database of Ref. [12].

LES Case	M_{jet}	T_{jet}/T_{∞}	M_a	Re_{jet}
B118	1.5	1.0	1.5	300,000
B122	1.5	1.74	1.98	155,000

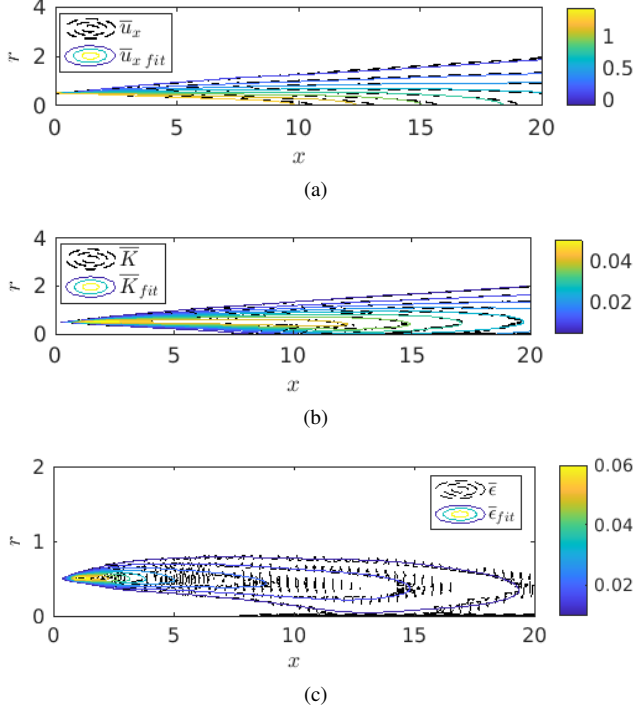


Figure 1: Comparison of computed and fitted contours of the mean values of (a) streamwise velocity \bar{u}_x , (b) TKE \bar{K} , and (c) dissipation $\bar{\epsilon}$, all for the B118 jet.

was interpolated to a cylindrical structured grid having about 1.3 million points.

Although the LES used a larger computational domain, for the present work we restricted the streamwise extent to $20D_j$ and the radial extent of $3.5D_j$. The calculation of the Green's function requires the mean streamwise velocity \bar{u}_x and density $\bar{\rho}$. Contours of the former are shown in fig. 1(a) for the isothermal B118 jet. Since radial derivatives of this are needed, we fit each radial profile of \bar{u}_x with a truncated Gaussian function of the form proposed originally in Ref. [15], and in turn smooth the Gaussian function's fit parameters with cubic splines [16]. As shown in the same figure, the fitted result matches well the original. Similar smoothing is pursued for the mean density field as well.

Using \bar{u}_x and $\bar{\rho}$ as input, the vector Green's functions of the LEE are computed with a code written in MATLAB following the theory laid out in the preceding section.

Source model 2 needs the mean TKE and dissipation fields; these are shown in Figures 1(b) and 1(c) for the B118 jet. To avoid spurious artifacts, these are also smoothed, this time using dual Gaussian functions at each axial station. The same figures demonstrate that negligible information is lost

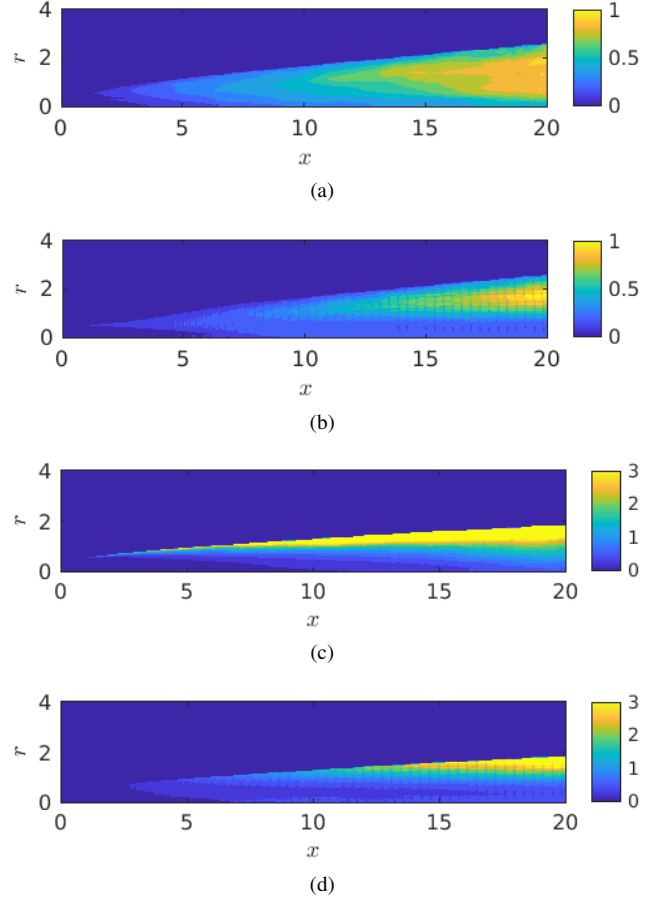


Figure 2: Comparison of length scales computed for the B122 jet using (a) cross-correlations (i.e., source model 1), and (b) $\bar{K} - \bar{\epsilon}$ (i.e., source model 2). Comparison of time scales computed for the B122 jet using (c) cross-correlations (i.e., source model 1), and (d) $\bar{K} - \bar{\epsilon}$ (i.e., source model 2).

in this process.

The length and time scales computed using the first source model (i.e., from the cross-correlation data) are presented in figs. 2(a) and 2(c) respectively for the heated B122 jet. Equation (9b) shows that the noise source itself vanishes in regions where the velocity scale (and so the TKE) vanishes, which happens outside the shear layer. Thus, the turbulent scales are not computed in these regions; hence, they appear uniformly deep blue in the filled contour plots of fig. 2. The shear layer starts out being very thin near the nozzle exit and thickens as one moves downstream. Because of this, the turbulent structures are also increasing in size as one progresses downstream, which is in turn reflected in the length scales shown in fig. 2(a). Since larger structures have greater temporal persistence, the time scales also increase as one goes downstream, and especially near the outer edge of the shear layer.

Importantly for the purposes of the present work, a comparison of figs. 2(a) and 2(b) confirms that the two

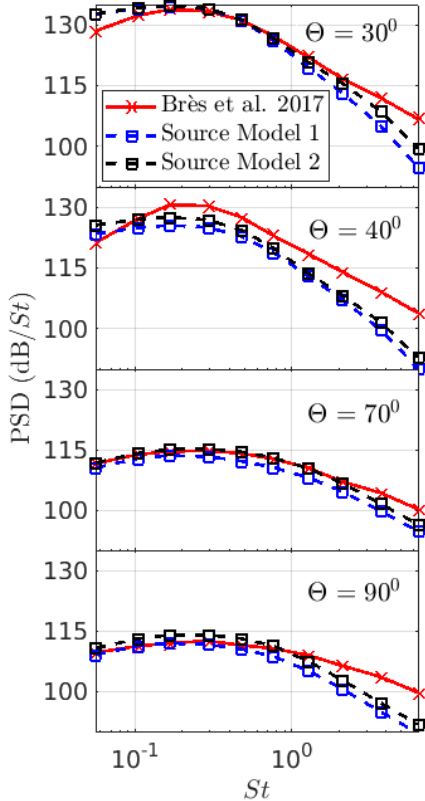


Figure 3: Comparison of the far-field noise predicted with the FW-H results (B118).

source models predict qualitatively similar length scales having the same order of magnitude, although there are some subtle differences. Similarly, a study of figs. 2(c) and 2(d) confirms that the time scales obtained from the two approaches are also similar. To obtain the length and time scales from source model 2, we need to specify the corresponding coefficients. To obtain the match seen in these figures, these were chosen as

$$c_\ell = 1.2, \quad c_\tau = 0.18. \quad (16)$$

Note that both these are three times higher than the values used in Ref. [11].

Of course, source model 2 is the only one that is applicable when the input data is a steady RANS solution. Its agreement with the results from the source model 1 shown here, independently validates it using the greater wealth of information available in the present LES database.

The far-field noise is quantified using the sound pressure level (SPL) spectra at various polar angles. The polar radii of these observer positions are chosen to match the location of microphones in the reference experiments of Ref. [17], wherein a rectilinear array was used. The reference noise spectra figs. 3 and 4 for the two jets are calculated directly from the time-resolved flow field fluctuation data available in the LES solutions of Ref. [12]. For this, the Ffowcs Williams and Hawkins (FW-H) method [18] is used, as was done in

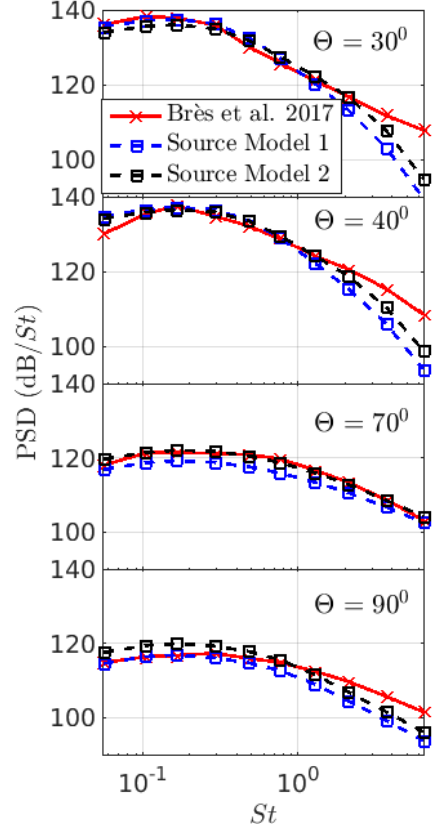


Figure 4: Comparison of the far-field noise predicted with the FW-H results (B122).

Ref. [12]. The authors reported excellent match with the reference spectral data from the experiments of Ref. [17], which validated their LES simulations.

Results from our two different source models are juxtaposed with the reference spectra in figs. 3 and 4, and they are essentially identical. Moreover, the comparison with the reference spectra is excellent, except at high frequencies. It is evident that our severely approximate models perform very satisfactorily vis-à-vis the much more input-heavy reference approach. To obtain these spectral agreement, we consistently set the remaining parameters that are common to our two models. That is, only one value was used for each parameter across both the jets, and definitely in calculations across all observer locations. These values were

$$B_0 = 0.451, \quad B_{>0} = 4.51, \quad c_u = 1. \quad (17)$$

The first two values are about twice of those reported by Ref. [11]; the last one matches the reference.

IV. CONCLUSIONS

This paper explains an existing methodology for the prediction of jet noise based on steady RANS data. The Euler equations are rearranged into a noise propagation operator and noise sources. The propagation operator is simplified to a third-order partial differential equation (PDE) of a single variable – the Lilley’s operator – based on the locally-parallel

mean flow assumption. The scalar Green’s function of Lilley’s operator is computed numerically using the adjoint approach. Subsequently, the vector Green’s functions of the LEE are recovered from the Lilley’s Green’s function.

On the source side, two noise source models are used in this work. One uses the local values of the mean turbulent kinetic energy \bar{K} and dissipation $\bar{\epsilon}$; these quantities are readily available from steady $K - \epsilon$ RANS simulations. Results from this are compared with another source model that relies on knowledge of the spatio-temporal cross-correlation of the streamwise velocity – information that can only be found from an LES or a DNS database. To enable a comparison of the two models, we used the well-validated LES database of Ref. [12] comprising of an isothermal and a heated Mach 1.5 jets. This work validates the former low-input-burden noise source model against the latter high-input-burden model results using this LES database. Specifically, the turbulent length and time scales computed from the two models demonstrate very similar spatial trends – both qualitatively and quantitatively.

The similarity of the outcomes from the two source models in the near-field region is reflected in the equivalence of their far-field sound predictions also. Moreover, both models show very encouraging agreement with the much more high-input burden FW-H results that required the time-resolved LES solution itself.

NOMENCLATURE

p	Pressure
\mathbf{u}	Velocity vector
a	Local speed of sound
t	Time
γ	Specific heat ratio
f_0	Unsteady dilatation
\mathbf{f}	Unsteady force vector per unit mass
\mathbf{x}	Position vector
ω	Radial frequency
δ	Dirac delta function
δ_{ij}	Kronecker delta function
L_L	Lilley’s operator
\hat{g}	Green’s function of L_L
S_p	Spectral density
τ	Time lag
$\boldsymbol{\eta}$	Spatial lag vector
R	Polar radius of the observer
Θ	Polar angle of the observer
B_n	Amplitude constants for various n
St	Strouhal number
D_j	Jet diameter
U_j	Jet exit velocity
τ_s	Turbulent time scale
ℓ_i	Turbulent length scale
u_s	Turbulent velocity scale
K	Turbulent kinetic energy
ϵ	Dissipation
$\overline{(\cdot)}$	Time-averaged quantity

$(\cdot)'$	Perturbation quantity
$\overline{(\cdot)}$	Temporal Fourier-transformed quantity
$(\cdot)^*$	Complex conjugate
$(\cdot)_\infty$	Freestream quantity
$(\cdot)_s$	Source quantity
$\langle\langle\cdot\rangle\rangle$	Ensemble average
$(\cdot)_g^n$	n th component of vector Green’s function

ACKNOWLEDGEMENTS

The authors are grateful to Guillaume Brès for sharing the LES solutions for the two supersonic jets, without which this work would not have been possible. Funding from a research grant from Indian Space Research Organization is also gratefully acknowledged.

REFERENCES

- [1] C. K. W. Tam and P. Chen. Turbulent mixing noise from supersonic jets. *AIAA Journal*, 32(9):1774–1780, 1994.
- [2] M. J. Lighthill. On sound generated aerodynamically i. general theory. *Proceedings of the Royal Society of London A*, 211(1107):564–587, 1952.
- [3] G. M. Lilley. On the noise from jets. Technical Report CP-131, AGARD, 1974.
- [4] M. E. Goldstein. A generalized acoustic analogy. *Journal of Fluid Mechanics*, 488:315–333, 2003.
- [5] C. K. W. Tam and L. Auriault. Jet mixing noise from fine-scale turbulence. *AIAA Journal*, 37(2):145–153, 1999.
- [6] P. J. Morris and F. Farassat. Acoustic analogy and alternative theories for jet noise prediction. *AIAA Journal*, 40(4):671–680, 2002.
- [7] P. J. Morris and S. Boluriaan. The prediction of jet noise from CFD data. In *10th AIAA/CEAS Aeroacoustics Conference, paper 2977*, 2004.
- [8] N. Raizada and P. J. Morris. Prediction of noise from high speed subsonic jets using an acoustic analogy. In *12th AIAA/CEAS Aeroacoustics Conference, paper 2596*, 2006.
- [9] T. F. Balsa. The far field of high frequency convected singularities in sheared flows, with an application to jet-noise prediction. *Journal of Fluid Mechanics*, 74(2):193–208, 1976.
- [10] M. E. Goldstein. *Aeroacoustics*. McGraw-Hill Book Co., New York, 1976.
- [11] S. A. E. Miller. Toward a comprehensive model of jet noise using an acoustic analogy. *AIAA Journal*, 52(10):2143–2164, 2014.
- [12] G. A. Brès, F. E. Ham, J. W. Nichols, and S. K. Lele. Unstructured large-eddy simulations of supersonic jets. *AIAA Journal*, 55(4):1164–1184, 2017.
- [13] H. S. Ribner. The generation of sound by turbulent jets. In *Advances in Applied Mechanics*, volume 8, pages 103–182. Elsevier, 1964.
- [14] P. J. Morris and K. B. M. Q. Zaman. Velocity measurements in jets with application to noise source modeling. *Journal of Sound and Vibration*, 329(4):394–414, 2010.

- [15] T. R. Troutt and D. K. McLaughlin. Experiments on the flow and acoustic properties of a moderate-Reynolds-number supersonic jet. *Journal of Fluid Mechanics*, 116:123–156, 1982.
- [16] K. Gudmundsson. *Instability wave models of turbulent jets from round and serrated nozzles*. PhD thesis, California Institute of Technology, 2010.
- [17] R. Schlinker, J. Simonich, R. Reba, T. Colonius, and F. Ladeinde. Decomposition of high speed jet noise: Source characteristics and propagation effects. In *14th AIAA/CEAS Aeroacoustics Conference, paper 2890*, 2008.
- [18] J. E. Ffowcs Williams and D. L. Hawkings. Sound generation by turbulence and surfaces in arbitrary motion. *Philosophical Transactions of the Royal Society of London A*, 264:321–342, 1969.